Exploiting the information content of dipolar couplings: determination of the temperature dependence of the inter-ring twist angle of biphenyl dissolved in uniaxial mesophases

G. Celebre[a]; G. De Luca[a]; M. Longeri[a]

[a] Dipartimento di Chimica, Università della Calabria, Rende, (CS), Italy

PLEASE SCROLL DOWN FOR ARTICLE

INVITED ARTICLE

Exploiting the information content of dipolar couplings: determination of the temperature dependence of the inter-ring twist angle of biphenyl dissolved in uniaxial mesophases

G. Celebre, G. De Luca and M. Longeri*

Dipartimento di Chimica, Università della Calabria, Rende (CS), Italy

In the present work, the quite intriguing question of the temperature dependence of the inter-ring angle of biphenyl in fluid condensed phases has been investigated by the proton liquid crystal nuclear magnetic resonance technique. The spectra of the molecule dissolved in three different thermotropic uniaxial solvents (one of which shows also a smectic A phase) at different values of temperature have been analysed by standard procedures, and the resulting temperature-dependent dipolar coupling sets have been rationalised by the additive potential for the treatment of the ordering interactions method, combined with the direct probability description of the torsional curve, in order to obtain the distribution of the twist angle φ for each temperature. The results emphasise a very slight but unequivocal and systematic increase of φ_M (the most probable value of the dihedral angle) with temperature, so qualitatively confirming what was previously found by a cruder hybrid approach (based on experimental quadrupolar splittings of perdeuteriated biphenyl combined with computer-simulated order parameters) carried out by two of the present authors (Celebre, G.; De Luca, G.; Mazzone, G. *J. Mol. Struct. (THEOCHEM)* **2005**, *728*, 209–214).

Keywords: biphenyl; NMR; liquid crystals; conformational analysis; AP method; direct probability distribution

1. Introduction

The biphenyl molecule can be seen as a building block for the rigid core of many mesogenic compounds [1] and liquid-crystalline or semi-crystalline aromatic polymers [2]. The dihedral angle, φ, between the two phenyl rings plays an important role in determining the physical properties of such materials and their molecular packing. Moreover, since biphenyl is a molecule interesting and fascinating in itself, it has been the object, over many years, of many studies, both experimental [3–13] and theoretical [14–16]. Such interest is mainly due to its relatively simple structure and to the strong conformational dependence of the molecule on the phase of the material. As a matter of fact, the value of φ_M (henceforth, φ_M will denote the global minimum of the torsional potential or, equivalently, the most probable value of the twist angle, see Figure 1) was found to be about 45° in the gas phase (electron diffraction studies [3] and theoretical calculations [14]) and 0° (coplanar rings) or 10–15° in the crystalline phase (X-ray studies [3–7] and ^{13}C solid state nuclear magnetic resonance (NMR) techniques [8, 9]). In solution, the situation is more complex: the φ_M angle is commonly believed to be in the range of 30–40° [9–12] but also lower values ($\sim$20°) have been reported [17]. The determination of the conformational equilibrium and especially the temperature dependence of the inter-ring angle of the biphenyl molecule are thus particularly interesting. In this context, NMR spectroscopy in liquid-crystalline solvents (LXNMR) has proved to be a particularly effective and elegant technique with which to study the conformational distribution of solutes. Several ^{1}H-LXNMR studies of the conformational distribution of biphenyl and biphenyl derivatives as solutes in different ordered fluid phases have been reported in the literature [18–21]. In these previous studies the authors report values for φ_M in the range 33.1–37.6°, depending on the method chosen for the analysis of the experimental parameters, represented by the dipolar (or direct) interproton couplings D_{HH}. The single-quantum spectrum of the biphenyl molecule, a *ten-spin* system, is quite complicated: this is basically the reason why all of the ^{1}H spectra studied in the literature [18, 19] have been recorded at just one fixed temperature (about room temperature). In several papers, the inter-ring angle has been studied for a few different temperatures [21] and in different nematic solvents [22], but these works mainly deal with simpler systems represented by para-disubstituted biphenyls (a detailed comparison between the final considerations of [21] and those of the present work concerning the effect of temperature on the conformational equilibrium will be given in Section 4). The variation of the biphenyl φ_M angle with temperature (from 17°C to 33 °C) has been specifically investigated by Celebre *et al.* [23] using a hybrid set of data, obtained from a combination of the experimental quadrupolar splittings of perdeuteriated biphenyl in the 55wt% ZLI1132/EBBA magic [24] nematic mixture (MM), with

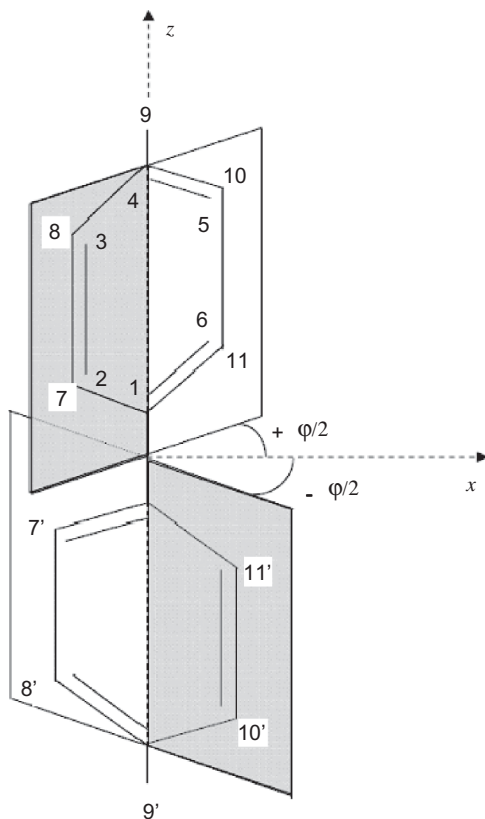*Corresponding author. Email: m.longeri@unical.it

Figure 1. The biphenyl molecule with the coordinate system and atomic labelling.

computer-simulated realistic orientational information predicted by a so-called box modelling of the molecule [25, 26]. The results seem to indicate a slight increase in φ_M with temperature. Even though the values of φ_M obtained by this approach were affected by large errors, this intriguing result prompted us to undertake more reliable ^{1}H-LXNMR experiments in order to investigate in detail this phenomenon. Thus, in the present work the problem has been tackled by determining a large number of new sets of experimental D_{HH} data for the biphenyl molecule dissolved in three different uniaxial thermotropic liquid crystals solvents, at various temperatures (one of the solvents also shows a smectic A phase below its nematic range). The AP-DPD method (Additive Potential for the treatment of the ordering interactions, combined with the Direct Probability Description of the torsional curve [27]) has been used to obtain the twist-angle distribution for each temperature; moreover, the use of three different solvents has also allowed us to test how much the nature of the solvent affects the results.

2.   Experimental

Three approximately 10 wt% solutions were prepared by dissolving biphenyl (commercially available from Aldrich) in the nematic solvents I52 (from Merck) and MM (ZLI1132 from Merck; EBBA from standard synthesis procedures [28, 29]); and in HAB (Merck), exhibiting nematic and smectic A phases depending on the working temperature (the pure solvent shows a nematic phase between 349 K and 331 K, and a smectic A phase at temperatures lower than 331 K [30]). In Figure 2 the molecular structures of the solvents are shown. In order to avoid confusion and misunderstanding, we would like to emphasise that in this paper we will call HAB the 4,4'-di-*n*-heptylazoxybenzene molecule, as reported elsewhere [30], and not the 4,4'-di-*n*-heptyloxyazoxybenzene, as usually understood by using this acronym (see, for example, the free version of LiqCryst Online 1999 Database [31] and the references therein).

The samples were heated a few times up to their nematic–isotropic transition temperature, T_{NI}, strongly shaken to homogenise the solutions, and left to cool slowly in the magnetic field of the NMR spectrometer. The ^{1}H-spectra were then recorded within 40–50 min intervals of thermostatisation for each temperature, the temperature values were properly chosen to compare effectively the stable biphenyl conformations in the three solvents at quite similar reduced temperatures, $T_{red} = T/T_{NI}$. In practice, the working temperatures ranged from 290 K to 320 K in I52, from 280 K to 310 K in MM and from 300 K to 315 K in HAB: these ranges, in terms of T_{red}, correspond to 0.84–0.93 for I52 and MM solutions and 0.88–0.93 for the HAB solution. We note that these latter values correspond to a $T_{NI} \sim$ 340 K, which is very much lower than that reported in the literature [30] and given here for the pure solvent: this is, of course, mainly due to the relatively high concentration of the solute, and because the starting purity of the solvent we used was not particularly high. All of the spectra were recorded on a Bruker Avance 500 MHz (11.74 T) instrument, equipped with a Bruker BVT 2000 temperature control unit. The analyses of the proton spectra were carried out using a home-made iterative computer program called ARCANA [32] and the resulting dipolar couplings are reported in Tables 1, 2 and 3, for biphenyl in I52, in MM and in HAB, respectively. In Figure 3, the calculated and experimental proton spectra of biphenyl in I52 at 305 K are shown as an example.

3.   Theory

In a uniaxial liquid-crystalline environment where the director aligns along the external applied magnetic field (as for the liquid-crystalline solvents used here), the D_{ij} dipolar coupling between the *i*th and *j*th nuclei of a flexible molecule with just one torsional degree of freedom, φ, can be written as
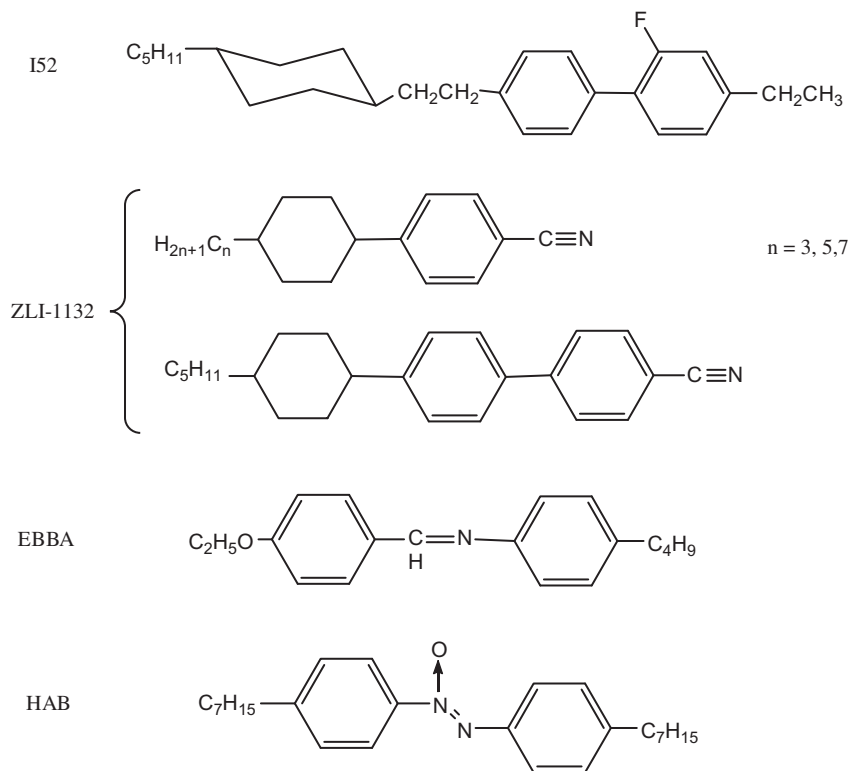
Figure 2.   Chemical structures of the liquid-crystalline solvents used in the present work.

Table 1. Observed dipolar couplings D_{ij} and chemical shift differences of biphenyl in I52 at different temperatures (see Figure 1 for the atom numbering).

	$T = 290$ K ($T_{red} = 0.840$)	$T = 305$ K ($T_{red} = 0.884$)	$T = 310$ K ($T_{red} = 0.898$)	$T = 320$ K ($T_{red} = 0.927$)
$D_{7,8}$/Hz	-3714.59 ± 0.04	-3504.95 ± 0.03	-3431.37 ± 0.04	-3275.15 ± 0.04
$D_{7,9}$/Hz	-460.28 ± 0.11	-435.83 ± 0.09	-427.20 ± 0.12	-408.76 ± 0.11
$D_{7,10}$/Hz	15.65 ± 0.05	11.44 ± 0.04	10.40 ± 0.05	7.56 ± 0.06
$D_{7,11}$/Hz	261.28 ± 0.13	240.57 ± 0.11	233.73 ± 0.16	218.70 ± 0.14
$D_{7,7'}$/Hz	-1192.08 ± 0.10	-1114.15 ± 0.07	-1087.04 ± 0.12	-1030.34 ± 0.09
$D_{7,8'}$/Hz	-311.15 ± 0.05	-293.41 ± 0.03	-287.39 ± 0.04	-274.20 ± 0.04
$D_{7,9'}$/Hz	-217.74 ± 0.11	-205.42 ± 0.09	-201.47 ± 0.10	-192.54 ± 0.10
$D_{8,9}$/Hz	98.57 ± 0.10	69.45 ± 0.09	60.68 ± 0.13	41.30 ± 0.11
$D_{8,10}$/Hz	261.09 ± 0.15	240.46 ± 0.12	232.67 ± 0.17	217.94 ± 0.15
$D_{8,8'}$/Hz	-117.41 ± 0.12	-110.49 ± 0.07	-108.22 ± 0.12	-103.28 ± 0.11
$D_{8,9'}$/Hz	-88.86 ± 0.10	-84.95 ± 0.09	-83.79 ± 0.13	-80.31 ± 0.11
$D_{9,9'}$/Hz	-70.90 ± 0.07	-66.71 ± 0.06	-65.27 ± 0.07	-62.17 ± 0.07
$(v_7 - v_9)$/Hz	-495.07 ± 0.09	-462.94 ± 0.08	-455.76 ± 0.11	-430.98 ± 0.09
$(v_8 - v_9)$/Hz	-441.01 ± 0.11	-414.22 ± 0.08	-403.06 ± 0.10	-382.59 ± 0.11

$$D_{ij} = \frac{2}{3} \int P_{LC}(\Omega, \varphi) \, D_{ij}(\Omega, \varphi) \, d\Omega \, d\varphi, \qquad (1)$$

where $D_{ij}(\Omega, \varphi)$ is

$$D_{ij}(\Omega, \varphi) = \langle \mathbf{s}(\Omega) : \mathbf{D}_{ij}(\varphi) \rangle. \qquad (2)$$

Here Ω denotes the set of angles needed to give the orientation of the mesophase director **n** in the chosen

molecular frame and the angular brackets $\langle ... \rangle$ indicate the statistical average over the small-amplitude high-frequency molecular vibrational modes (torsion φ excluded) and the symbol ':' represents the *double dot* or *inner* product of the two tensors. We now give a detailed description of the ingredients of Equations (1) and (2). (1) The elements of the tensor, $\mathbf{s}(\Omega)$, correspond to

$$s_{ab}(\Omega) = \frac{3 \, \cos \omega_a \cos \omega_b - \delta_{ab}}{2}, \qquad (3)$$

Table 2. Observed dipolar couplings D_{ij} and chemical shift differences of biphenyl in MM at different temperatures (see Figure 1 for the atom numbering).

	$T = 280$ K ($T_{red} = 0.838$)	$T = 285$ K ($T_{red} = 0.853$)	$T = 300$ K ($T_{red} = 0.898$)	$T = 310$ K ($T_{red} = 0.928$)
$D_{7,8}$/Hz	-3470.01 ± 0.04	-3452.70 ± 0.05	-2641.81 ± 0.06	-1930.92 ± 0.07
$D_{7,9}$/Hz	-432.66 ± 0.10	-430.15 ± 0.12	-332.91 ± 0.16	-246.76 ± 0.22
$D_{7,10}$/Hz	8.57 ± 0.05	8.41 ± 0.06	-0.58 ± 0.10	-4.70 ± 0.10
$D_{7,11}$/Hz	231.95 ± 0.12	231.54 ± 0.11	163.50 ± 0.21	111.35 ± 0.26
$D_{7,7'}$/Hz	-1174.07 ± 0.09	-1166.17 ± 0.12	-866.99 ± 0.17	-624.65 ± 0.16
$D_{7,8'}$/Hz	-293.68 ± 0.04	-292.38 ± 0.05	-224.08 ± 0.08	-164.06 ± 0.07
$D_{7,9'}$/Hz	-203.51 ± 0.09	-202.26 ± 0.11	-156.40 ± 0.16	-114.41 ± 0.21
$D_{8,9}$/Hz	49.24 ± 0.09	49.12 ± 0.12	-16.31 ± 0.18	-40.72 ± 0.21
$D_{8,10}$/Hz	231.52 ± 0.14	229.98 ± 0.19	161.56 ± 0.25	111.30 ± 0.26
$D_{8,8'}$/Hz	-110.12 ± 0.10	-109.44 ± 0.14	-84.11 ± 0.20	-60.58 ± 0.16
$D_{8,9'}$/Hz	-83.47 ± 0.10	-83.18 ± 0.12	-63.84 ± 0.19	-46.89 ± 0.20
$D_{9,9'}$/Hz	-66.04 ± 0.07	-65.50 ± 0.08	-49.89 ± 0.10	-36.88 ± 0.13
$(v_7 - v_9)$/Hz	-441.68 ± 0.09	-439.78 ± 0.12	-308.04 ± 0.16	-202.50 ± 0.23
$(v_8 - v_9)$/Hz	-389.04 ± 0.10	-392.54 ± 0.13	-289.22 ± 0.16	-196.08 ± 0.20

Table 3. Observed dipolar couplings D_{ij} and chemical shift differences of biphenyl in HAB at different temperatures (see Figure 1 for the atom numbering).

	$T = 300$ K ($T_{red} = 0.882$)	$T = 305$ K ($T_{red} = 0.897$)	$T = 310$ ($T_{red} = 0.912$)	$T = 315$ ($T_{red} = 0.926$)
$D_{7,8}$/Hz	-2789.27 ± 0.09	-2607.77 ± 0.02	-2386.36 ± 0.09	-2114.86 ± 0.16
$D_{7,9}$/Hz	-350.25 ± 0.07	-326.81 ± 0.08	-300.74 ± 0.25	-266.56 ± 0.58
$D_{7,10}$/Hz	3.58 ± 0.10	2.28 ± 0.03	1.16 ± 0.14	-1.81 ± 0.23
$D_{7,11}$/Hz	180.92 ± 0.09	165.81 ± 0.09	149.70 ± 0.34	128.62 ± 0.46
$D_{7,7'}$/Hz	-911.68 ± 0.06	-848.77 ± 0.06	-772.07 ± 0.21	-677.29 ± 0.34
$D_{7,8'}$/Hz	-235.99 ± 0.03	-220.22 ± 0.03	-200.84 ± 0.10	-179.74 ± 0.19
$D_{7,9'}$/Hz	-163.66 ± 0.07	-153.99 ± 0.07	-140.36 ± 0.24	-126.91 ± 0.48
$D_{8,9}$/Hz	11.77 ± 0.09	-0.12 ± 0.07	-8.88 ± 0.30	-20.89 ± 0.77
$D_{8,10}$/Hz	178.65 ± 0.15	165.19 ± 0.10	146.55 ± 0.38	129.97 ± 0.60
$D_{8,8'}$/Hz	-88.60 ± 0.06	-82.75 ± 0.06	-77.00 ± 0.25	-68.01 ± 0.48
$D_{8,9'}$/Hz	-66.87 ± 0.07	-62.87 ± 0.07	-59.93 ± 0.30	-50.27 ± 0.66
$D_{9,9'}$/Hz	-53.69 ± 0.09	-49.94 ± 0.04	-45.13 ± 0.15	-39.47 ± 0.29
$(v_7 - v_9)$/Hz	-314.80 ± 0.10	-293.09 ± 0.07	-258.55 ± 0.25	-210.21 ± 0.33
$(v_8 - v_9)$/Hz	-300.25 ± 0.13	-278.01 ± 0.07	-252.74 ± 0.23	-214.36 ± 0.50
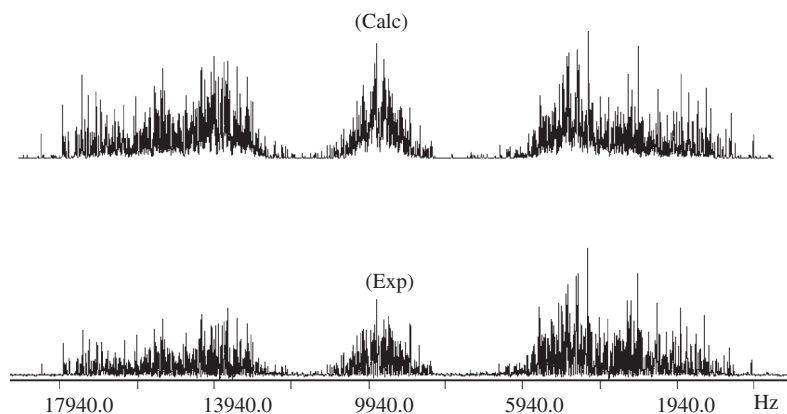
Figure 3.   500 MHz experimental and calculated ^{1}H spectrum of biphenyl dissolved in I52 at 305 K.

where ω_a is the instantaneous angle between **n** and the *a* axis of a Cartesian coordinate system (*a,b,c*) fixed on the solute molecule, and δ_{ab} is the Kronecker delta function. (2) The term $\mathbf{D}_{ij}(\varphi)$ is the geometry-dependent dipolar coupling tensor expressed in the molecular frame:

$$D_{ij}^{ab}(\varphi) = -K_{ij} \frac{3\cos\theta_a(\varphi)\cos\theta_b(\varphi) - \delta_{ab}}{r_{ij}^3(\varphi)} \ , \qquad (4)$$

where $r_{ij}(\varphi)$ is the φ-dependent *i–j* internuclear distance, $\theta_a(\varphi)$ is the conformation dependent angle between the *a*-axis of the molecular frame and the $\mathbf{r}_{ij}(\varphi)$ vector connecting the nuclei *i* and *j*, and K_{ij} is given by

$$K_{ij} = \frac{\mu_0 \hbar \gamma_i \gamma_j}{16\pi^2} \qquad (5)$$

where $\hbar = \frac{h}{2\pi}$ (*h* is the Planck constant), γ is the nuclear magnetogyric ratio and μ_0 is the vacuum magnetic permeability.

(3) The function $P_{LC}(\Omega, \varphi)$ describes the properly normalised orientational-conformational probability distribution function of the solute in the liquid-crystalline environment. It can be defined as [33, 27]

$$P_{LC}(\Omega, \varphi) = P_\varphi(\varphi) P_\Omega(\Omega, \varphi), \qquad (6)$$

where

$$P_\Omega(\Omega, \varphi) = \frac{\exp[-U_{\text{ext}}(\Omega, \varphi)/k_B T]}{Q} \qquad (7)$$

with

$$Q = \int \exp[-U_{\text{ext}}(\Omega, \varphi)/k_B T]\, d\Omega \, d\varphi. \qquad (8)$$

Here k_B is the Boltzmann constant. $U_{\text{ext}}(\Omega, \varphi)$ is a purely anisotropic external orientational potential which, in the frame of the Additive Potential (AP) method [34, 35], can be described as

$$\begin{aligned} U_{\text{ext}}(\Omega, \varphi) = &-\varepsilon_{2,0}(\varphi)\, C_{2,0}(\Omega) \\ &- 2\text{Re}\left(\varepsilon_{2,2}(\varphi)\right)\text{Re}\left(C_{2,2}(\Omega)\right), \end{aligned} \qquad (9)$$

where the $C_{2,m}(\Omega)$ are modified spherical harmonics [36], and the $\varepsilon_{2,m}(\varphi)$ are the elements of suitable

conformation-dependent solute–solvent interaction tensors. The peculiar feature of the AP method is that the $\varepsilon_{2,m}(\varphi)$ elements are constructed as a sum of conformationally-independent terms $\varepsilon_{2,p}(l)$ representing the single contributions of each rigid fragment, *l*, in the molecule to the total interaction tensor,

$$\varepsilon_{2,m}(\varphi) = \sum_l \sum_p \varepsilon_{2,p}(l) D_{p,m}^2(\Lambda_\varphi^l). \qquad (10)$$

In this equation, the second-rank Wigner rotation matrix $D_{p,m}^2(\Lambda_\varphi^l)$ [36] relates the conformation-dependent Λ_φ^l orientation of the *l*th molecular sub-unit to the molecule-fixed reference frame. Essentially, the $\varepsilon_{2,p}(l)$ are unknown quantities whose values are adjusted to produce the best agreement with the experimental data. In the AP-DPD method, the $P_\varphi(\varphi)$ of Equation (6) can be written as [27]

$$P_\varphi(\varphi) = P_{\text{iso}}(\varphi) \frac{W(\varphi) Z_{\text{iso}}}{Z}, \qquad (11)$$

where

$$W(\varphi) = \int \exp[-U_{\text{ext}}(\Omega, \varphi)/k_B T]\, d\Omega, \qquad (12)$$

$$Z = \int W(\varphi) \cdot P_{\text{iso}}(\varphi)\, d\varphi \qquad (13)$$

and

$$Z_{\text{iso}} = \int P_{\text{iso}}(\varphi)\, d\varphi. \qquad (14)$$

The distribution function $P_{\text{iso}}(\varphi)$ represents the real target of conformational studies in liquids [35]. Unlike $P_\varphi(\varphi)$, $P_{\text{iso}}(\varphi)$ is, in principle, free from possible conformational effects induced by the orientational ordering of the mesophase. So, it should be considered the real conformational distribution of our solute in a conventional liquid sharing, at the temperature studied, the same physical properties (determining the thermodynamics of the solution, as polarity, density etc.) of the liquid-crystalline solvent used, with the exception of the ordering strength. In the present case, the normalised $P_{\text{iso}}(\varphi)$ is modelled directly as a sum of Gaussian functions [27, 37–41]:

$$P_{\text{iso}}(\varphi) = \frac{\sum_{i=1}^{2} \exp\left[-\left(\frac{\varphi - ((-1)^i\,\varphi_M)}{\sigma}\right)^2 \Big/ 2\right] + \exp\left[-\left(\frac{\varphi - ((-1)^i(\pi - \varphi_M))}{\sigma}\right)^2 \Big/ 2\right]}{4\sigma\sqrt{2\pi}}. \qquad (15)$$

This function contains two unknowns: the most probable value of the twist angle φ_M, which is to be obtained by comparing the calculated with the observed dipolar couplings, and σ, representing the width at half maximum height.

Once our theoretical apparatus is fixed as we have described, we can proceed with the treatment. It is quite usual to assume that internal vibrations and overall reorientational (tumbling) motions of the molecule can be decoupled in Equation (2), because the dependence of $\mathbf{s}(\Omega)$ on the vibrational state of the molecule is believed to be small enough to be neglected to a good approximation (for more details about this point, see [42, 43, 27] and the references therein). Of course, this approximation could affect the results: in principle, very accurate determinations of the structure of solutes dissolved in liquid crystals should take into account vibration–reorientation coupling effects, besides the usual harmonic and anharmonic vibrational corrections. This is an old, well-known (and very complicated) problem, which has been treated in the past by many excellent authors [44–53]. Recently, the issue has received renewed attention [54–56]; in fact, in the present work (besides other approximations adopted to reduce the level of difficulties; see later) we have decided to ignore this point, relying on the fact that, presumably, our results and the consequent qualitative considerations should not be completely compromised by the assumptions. So, this implies that Equation (1) can be operationally re-written as

$$D_{ij} = \frac{2}{3} \int P_\varphi(\varphi) \sum_{a,b} S_{ab}(\varphi) \left\langle D_{ij}^{ab}(\varphi) \right\rangle d\varphi, \qquad (16)$$

where

$$S_{ab}(\varphi) = \frac{\int s_{ab}(\Omega) \, P_\Omega(\Omega, \varphi) \, d\Omega}{\int P_\Omega(\Omega, \varphi) \, d\Omega} \qquad (17)$$

are the familiar solute orientational order parameters, making up the well-known real symmetric traceless Saupe ordering matrix [57–59]. As anticipated previously, in treating the biphenyl molecule we have decided to adopt a series of other well-tested approximations (or assumptions) and convenient choices (also made in the past and recent studies of the same or similar systems [18–22, 40, 41]) in order to simplify the treatment of the problem:

(a) the vibrational corrections, quite unimportant for non-vicinal interproton dipolar couplings (as it is our case), have been neglected (as a matter of fact, it has been shown [60] that, in benzene, the harmonic vibrational correction for $^3D_{HH}$ is less than 2%, although it is well-known that an *apparent* solvent-dependent geometrical deformation of the ring could result [50, 51, 61]);

(b) the two phenyl ring fragments, in each solvent and at each temperature, keep a rigid C_{2v} symmetry structure as they rotate relative to each other;

(c) the molecular axis system for biphenyl, a molecule with D_2 symmetry when the inter-ring angle is different from 0° (where the molecule belongs to the D_{2h} point group) or 90° (D_{2d}), is chosen in such a way that the xz plane bisects the inter-ring angle, with z along the molecular long axis (see Figure 1; the y-axis, not shown, defines a right-handed Cartesian system). Such a frame is the Principal Axis System (PAS) for the $\mathbf{S}$ matrix, so that only two independent order parameters (namely, S_{zz} and $S_{xx}-S_{yy}$) are needed to describe completely the solute ordering.

Under the conditions (a), (b) and (c), the following explicit relation holds:

$$\begin{aligned}
\frac{2}{3}\sum_{a,b} &S_{ab}(\varphi)\left\langle D_{ij}^{ab}(\varphi)\right\rangle \\
&= -\frac{K_{ij}}{r_{ij}^3(\varphi)} \left[S_{zz}(\varphi)\left(3\cos^2\theta_z(\varphi) - 1\right) \right. \\
&\quad \left. + \left(S_{xx}(\varphi) - S_{yy}(\varphi)\right)\left(\cos^2\theta_x(\varphi) - \cos^2\theta_y(\varphi)\right) \right].
\end{aligned} \qquad (18)$$

As a consequence, Equation (16), giving the observed H–H dipolar coupling constants, can finally be written in the explicit form

$$\begin{aligned}
D_{ij} = \ -K_{ij} \int \frac{P_\varphi(\varphi)}{r_{ij}^3(\varphi)} \cdot &\left[S_{zz}(\varphi)\left(3\cos^2\theta_z(\varphi) - 1\right) + \right. \\
&\left. + \left(S_{xx}(\varphi) - S_{yy}(\varphi)\right)\left(\cos^2\theta_x(\varphi) - \cos^2\theta_y(\varphi)\right) \right] d\varphi \,. \quad (19)
\end{aligned}$$

The fragmental contributions, required to construct (via Equation (10)) the interaction tensors representing the coefficients of $U_{\text{ext}}(\Omega,\varphi)$ in Equation (9), were chosen to be those of the rings, $\varepsilon_{2,0}(R)$ and $\varepsilon_{2,2}(R)$. These, together with φ_M and σ of Equation (15) and the molecular structural features needed, represent the basic ingredients to calculate, respectively, the φ-dependent order parameters, the torsional probability distribution function and the geometrical contributions required by Equation (19). In our approach, the parameters ($\varepsilon_{2,0}(R)$, $\varepsilon_{2,2}(R)$, φ_M and σ, besides suitably chosen ring geometries; see Section 4) were varied in order to minimise the RMS error function:

$$\text{RMS} = \sqrt{\left.\sum_{i<j} \left[D_{ij}(\text{calculated}) - D_{ij}(\text{observed})\right]^2 \middle/ F\right.}, \quad (20)$$

where F represents the number of degrees of freedom (in terms of independent dipolar couplings) for the problem treated.

4. Results and discussion

The large number of dipolar couplings obtained from the analysis of the proton spectra, at different temperatures, for biphenyl in the three different liquid-crystalline solutions (12 D_{HH} for each solvent at each temperature, as reported in Tables 1–3) allowed us to establish: (i) the relative positions of the protons within each ring; (ii) the separation of the two rings and (iii) the inter-ring torsional distribution as a function of the temperature. By assuming a C_{2v} symmetry for the single rings and by considering the experimental intra-ring D_{HH} to be independent of φ, the intra-ring couplings can be used to determine the relative distances, r_{ij}, between the protons of a ring and the local order parameters, $S_{zz}(R)$ and $S_{xx}(R)$–$S_{yy}(R)$. Moreover, by making the further assumption that the ring geometries do not change significantly within the range of temperatures studied, a unique ring geometry for each solvent, common to all the temperatures studied in that mesophase, has been optimised from a simultaneous fit [37] to the total set of 24 intra-ring D_{HH} values (six intra-ring experimental D_{ij} for each of the four temperatures, for a total of 6 x 4 = 24 couplings in each solvent). Since only relative internuclear distances are available from experimental LXNMR data [62, 63], it is well-known that a fixed interproton distance is required; in this case, we decided to fix $r_{8,10}$ corresponding to the value for the canonical benzene ring. The relative geometries of the rings obtained for the three liquid-crystalline solutions are reported in Table 4 (where the regular ring and vibrationally corrected [19] geometries are also given for comparison). It is evident from Table 4 that the resulting biphenyl ring geometries in the three different nematic solvents studied are basically the same (within the experimental error), whereas they are slightly different (as reasonably expected) from those vibrationally corrected results of [19] (it is worth emphasising that the significant differences with respect to the reported regular geometries could probably be due, as said previously, to the neglect of

vibration–reorientation correlation effects [50, 51]). The local order parameters of the rings are reported in Table 5, where their third significant digits are affected by experimental errors which safely include the less-than-2% error [60] due to the neglect of harmonic vibrational corrections (note that in Table 3 of [19], where the harmonic vibrational corrections were applied, the order parameters are given, rightly, to the fourth significant digit). Finally, by assuming the ring geometries of Table 4 and by using all of the dipolar couplings available for each solvent at each temperature, we proceeded to determine simultaneously the φ-independent value of $r_{9,9'}$ (giving the information about the inter-ring distance) and, via Equations (11)–(15) (see Section 3), the twist angle distribution as a function of temperature. The user-friendly graphical program AnCon, developed by our group in the LXNMR_S.C.An. laboratory (Department of Chemistry) at the University of Calabria [64], has been used to perform the conformational analysis. The calculations were carried out by a simultaneous fit of the four temperature-dependent data sets for each solvent; then, each fitting target consisted of (12 D_{ij}) x (4 temperatures) = 48 D_{ij} couplings. The fitting procedure has been performed by adjusting the orientational and conformational parameters for a total of 14, that is, four pairs of $\varepsilon_{2,0}(R)$ and $\varepsilon_{2,2}(R)$ (one pair for each temperature), the value of φ_M for each temperature and a single value of $r_{9,9'}$ and σ (we assumed this to be common for all the temperatures) for each solvent. Summarising, the ratio (target D_{ij})/(adjustable parameters) = 48/14 assured us that the problems, were largely overdetermined. Finally, a good agreement between calculated and observed D_{HH} was obtained (from the fitting procedures described previously) for all three solutions: the resulting adjusted parameters and the RMS values are reported in Table 6. It is now worth emphasising that, although $P_{iso}(\varphi)$ is in principle different from $P_\varphi(\varphi)$ (see Equation (11)), for low ordered solutes, as is the case for this study, the two probability functions are practically

Table 4. Independent internuclear distance ratios adopted in this work for the ring protons for the biphenyl molecule dissolved in the three liquid-crystalline phases I52, MM and HAB (the last significant digits, in brackets, are all within the standard deviations). The values are compared with vibrationally corrected ([19], Table 3: Potential(I)) and regular (undistorted) benzene geometries.

	I52	MM	HAB	[19]	Regular
$r_{7,8}/r_{8,10}$	0.57(3)	0.57(3)	0.57(1)	0.568	0.577
$r_{7,9}/r_{8,10}$	0.99(8)	0.99(7)	0.99(6)	0.993	1
$r_{7,10}/r_{8,10}$	1.15(3)	1.15(3)	1.15(1)	1.150	1.155
$r_{7,11}/r_{8,10}$	1.00(0)	1.00(0)	0.99(7)	1.002	1
$r_{8,9}/r_{8,10}$	0.57(8)	0.57(8)	0.57(8)	0.577	0.577

Table 5. Local order parameters $S_{zz}(R)$ and $S_{xx}(R)$–$S_{yy}(R)$ obtained at each temperature from the procedure of ring structure optimisation for biphenyl dissolved in I52, MM and HAB.

	T/K			
	290	305	310	320
		I52		
$S_{zz}(R)$	0.465 ± 0.004	0.439 ± 0.006	0.430 ± 0.005	0.410 ± 0.004
$S_{xx}(R)$–$S_{yy}(R)$	0.117 ± 0.006	0.119 ± 0.008	0.119 ± 0.007	0.119 ± 0.006
	T/K			
	280	285	300	310
		MM		
$S_{zz}(R)$	0.435 ± 0.004	0.432 ± 0.004	0.332 ± 0.003	0.242 ± 0.002
$S_{xx}(R)$–$S_{yy}(R)$	0.126 ± 0.008	0.125 ± 0.006	0.101 ± 0.007	0.093 ± 0.005
	T/K			
	300	305	310	315
		HAB		
$S_{zz}(R)$	0.347 ± 0.005	0.324 ± 0.005	0.297 ± 0.004	0.263 ± 0.004
$S_{xx}(R)$–$S_{yy}(R)$	0.109 ± 0.008	0.105 ± 0.007	0.099 ± 0.006	0.097 ± 0.007

identical. So, in Figure 4 the probability distribution functions $P_\varphi(\varphi) \approx P_{iso}(\varphi)$, at the common T_{red} of 0.93 for biphenyl in the three different solvents, are shown.

Looking at the figure, it is possible to observe that the distribution functions differ perceptibly in the location of the maximum and have comparable heights. Finally, the resulting behaviour of φ_M versus T for all of the solutions is reported in Figure 5. Although, for experimental reasons, the temperature ranges considered in our study were quite restricted, a very slight but unequivocal and systematic increase of φ_M with temperature is observed: this confirms the trend crudely obtained in a previous paper by Celebre *et al.* [23]. In contrast, the quite similar slopes of the three curves highlight that the phenomenon is not very dependent on the nature of the solvent. In order estimate, albeit crudely, the sensitivity of the results obtained to our AP-DPD approach (which uses the $\boldsymbol{\varepsilon}(R)$ interaction tensors derived from the dipolar couplings which have not been corrected for all kinds of effects such as harmonic and anharmonic vibrational corrections, and effects due to vibration–reorientation interactions), the resulting uncertainties on $\varepsilon_{2,0}(R)$ and $\varepsilon_{2,2}(R)$ (apparently underestimated in Table 6) were deliberately increased by truncating the $\boldsymbol{\varepsilon}(R)$ values to the second significant digit. The trends of φ_M versus T_{red} obtained are very similar to those shown in Figure 5, and just slight differences (less than 1%, on average) were found on the single φ_M values.

Interestingly, in the study [21] (carried out by a maximum entropy (ME) analysis on 4,4'-dichlorobiphenyl (DCB) dissolved in I52 at 312 K, 322 K and 332 K) the effect of increasing the temperature was recognised by a broadening of the $P(\varphi)$ distribution function (see Figure 5 of [21]), with the ME-found φ_M being basically constant at 34° (in fact, within a ±1° of error, which could contain the variation we found in the present study for biphenyl in I52). Although a thermodynamic explanation is at first invoked by the authors of [21] to justify this effect, subsequently they conclude that the broadening observed with increasing temperature seems mostly due to a peculiar effect induced by the ME treatment, due to the decrease of the orientational order of the solute. In order to check the possibility of also rationalising the data of the present work by a broadening of the torsional curves, we performed a series of tests by considering σ (defining the width of the Gaussian curves) as a temperature-dependent adjustable parameter in our fittings, both adjusting or fixing the φ_M parameter in Equation (15). When we fix the dihedral φ_M at reasonably good values to represent the maximum probability (about a temperature-averaged φ_M value), leaving σ to change in order to minimise the RMS error as much as possible, we invariably obtain worse agreement with the experimental data; in contrast, when both σ and φ_M are left free to change, we observe a very slight increase of σ and, at the same time, basically the usual increase of φ_M shown in Figure 5. We proceeded also to analyse the data regarding DCB, given in [21], with our model, with

Table 6. The interaction parameters $\varepsilon_{2,0}(R)$ and $\varepsilon_{2,2}(R)$, the order parameters for the more stable conformation (corresponding to φ_M) and the values of σ, φ_M and $r_{9,9'}$ for biphenyl dissolved in I52, MM and HAB at different temperatures.

	T/K			
	290	305	310	320
		I52		
$\varepsilon_{2,0}(R)/RT$	1.395 ± 0.001	1.302 ± 0.001	1.270 ± 0.001	1.205 ± 0.001
$\varepsilon_{2,2}(R)/RT$	-0.611 ± 0.001	-0.572 ± 0.001	-0.557 ± 0.001	-0.529 ± 0.001
$S_{zz}(\varphi_M)$	0.465 ± 0.004	0.439 ± 0.006	0.430 ± 0.005	0.410 ± 0.004
$S_{xx}(\varphi_M)-S_{yy}(\varphi_M)$	0.145 ± 0.005	0.147 ± 0.006	0.147 ± 0.004	0.147 ± 0.006
$\sigma/°$		11.07 ± 0.15		
$r_{9,9'}/Å$		9.26 ± 0.01		
$\varphi_M/°$	36.18 ± 0.07	36.25 ± 0.08	36.28 ± 0.07	36.32 ± 0.07
RMS/Hz		0.52		

	T/K			
	280	285	300	310
		MM		
$\varepsilon_{2,0}(R)/RT$	1.293 ± 0.002	1.285 ± 0.002	0.951 ± 0.002	0.690 ± 0.002
$\varepsilon_{2,2}(R)/RT$	-0.582 ± 0.001	-0.576 ± 0.001	-0.403 ± 0.001	-0.270 ± 0.001
$S_{zz}(\varphi_M)$	0.435 ± 0.006	0.432 ± 0.005	0.331 ± 0.006	0.242 ± 0.005
$S_{xx}(\varphi_M)-S_{yy}(\varphi_M)$	0.153 ± 0.004	0.152 ± 0.004	0.140 ± 0.003	0.114 ± 0.004
$\sigma/°$		10.75 ± 0.20		
$r_{9,9'}/Å$		9.26 ± 0.01		
$\varphi_M/°$	35.07 ± 0.08	35.10 ± 0.08	35.31 ± 0.08	35.38 ± 0.08
RMS/Hz		0.52		

	T/K			
	300	305	310	315
		HAB		
$\varepsilon_{2,0}(R)/RT$	0.995 ± 0.002	0.927 ± 0.002	0.845 ± 0.002	0.747 ± 0.002
$\varepsilon_{2,2}(R)/RT$	-0.405 ± 0.002	-0.372 ± 0.002	-0.330 ± 0.002	-0.286 ± 0.002
$S_{zz}(\varphi_M)$	0.347 ± 0.007	0.324 ± 0.007	0.297 ± 0.006	0.263 ± 0.007
$S_{xx}(\varphi_M)-S_{yy}(\varphi_M)$	0.134 ± 0.006	0.130 ± 0.004	0.123 ± 0.005	0.114 ± 0.003
$\sigma/°$		11.75 ± 0.35		
$r_{9,9'}/Å$		9.24 ± 0.02		
$\varphi_M/°$	36.02 ± 0.15	36.03 ± 0.15	36.08 ± 0.15	36.17 ± 0.15
RMS/Hz		0.84		

the following results: $\varphi_M = 37.28°$ at 312 K, $\varphi_M = 37.39°$ at 322 K and $\varphi_M = 37.50°$ at 332 K, with the resulting $\sigma =15.1°$. Once again, a slight increase in φ_M with temperature can be appreciated. We think these results can lead us to conclude quite safely that an increase (even if very small) of φ_M with temperature is in any case required to reproduce closely the experimental data. The φ_M values found in this study for biphenyl are lower than the value of $\sim 37°$ previously obtained in two different solvents (ZLI1115 and I35) at room temperature, by making use of the AP model, but where the inter-ring potential was modelled as a two-term cosine expansion [18]. The same data in ZLI1115 and I35 (at room temperature), now revisited by us by using the AP-DPD description, lead to the following results: $\varphi_M(\text{ZLI1115}) = 35.42°$; $\varphi_M(\text{I35}) = 35.78°$. The result

$\varphi_M = 37.5°$ is common also to another study of biphenyl in MM [19], where an empirical formula for $S(\varphi)$ and (i) a discrete and (ii) a continuous description were used to model the inter-ring torsional potential. Our present φ_M values are also different from the values obtained previously ($\varphi_M = 34-35°$) by the ME analysis of the already available dipolar couplings for biphenyl in I35, ZLI1115 and MM [20]. Also in the just cited and discussed ME study of 4,4'-dichlorobiphenyl dissolved in I52 [21], the most probable value of the twist angle obtained was, as we have said, $\varphi_M = 34 \pm 1°$. More recently, a study on biphenyl and biphenyl derivatives in different nematic solvents by using the APME approach located the preferred inter-ring angle in the range 33–34° [22]. What we have said emphasises more and more the dependence of the results obtained on the method used to treat the
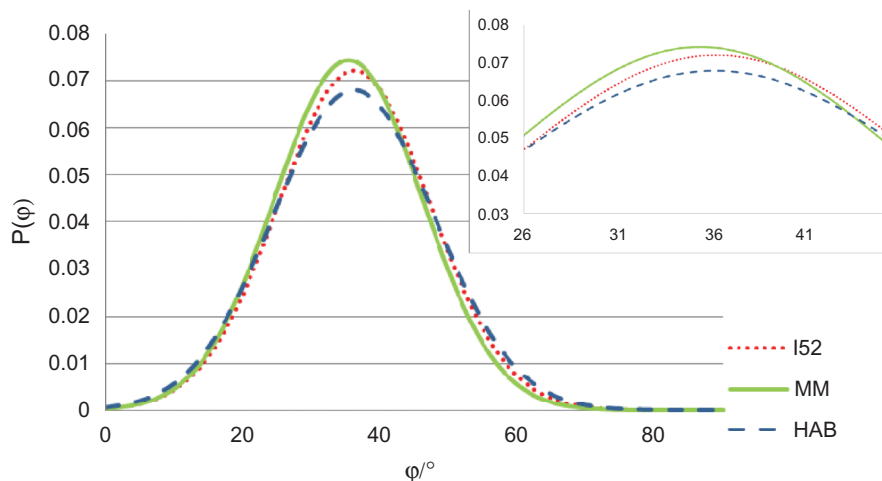
Figure 4. The probability distribution functions $P_\varphi(\varphi) \approx P_{iso}(\varphi)$ (compared at the common T_{red} of 0.93) for the biphenyl molecule in the three different solvents. In the inset, the location of the maxima is shown magnified (colour version online).
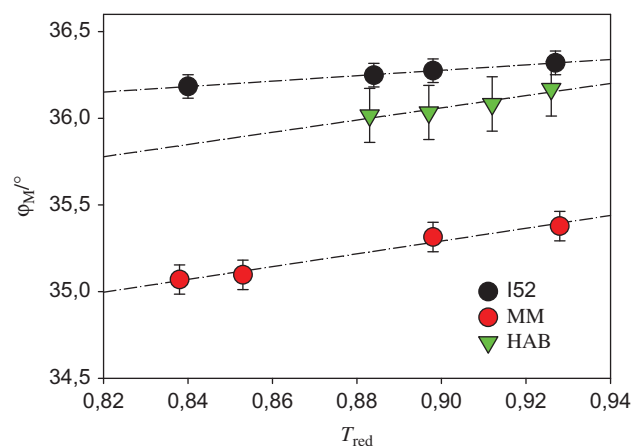

Figure 5. The behaviour of the most probable value of the twist angle φ_M versus T_{red} for biphenyl dissolved in I52, MM and HAB (colour version online).

experimental data. However, we are quite convinced that, once a certain model is chosen to treat the data, the subtle effect of the increasing trend of φ_M with temperature that we have found in this study should emerge also in other treatments (apart from possible peculiar features of the methods, as for the ME approach discussed): we hope the new experimental data presented in this work can also be studied by other approaches, to confirm or deny our guess.

5.   Conclusions

The power of the LXNMR technique and the high sensitivity of dipolar couplings to the conformational features of the solutes are, in our opinion, once again confirmed by the present work. Here, by using the AP-DPD approach to treat the experimental data, a small but experimentally detectable temperature-dependent shift toward higher dihedral angles at the maximum of the rotameric distribution of biphenyl in I52, MM and HAB has been found (in contrast, the role of the solvent in this phenomenon seems to be quite negligible). Of course, it has been emphasised that the absolute results depend significantly on the approach and the approximations chosen to analyse the data; in fact, we suppose that the subtle effects we have found should emerge also by making use of other models.

Acknowledgements

References

[1] Kelker, H.; Hatz, R. *Handbook of Liquid Crystals*; Verlag Chemie: Weinheim, 1980.
[2] Kovacic, P.; Jones, M.B. *Chem. Rev.* **1987**, *87*, 357–379.
[3] Almeniggen, A.; Bastiansen, O.; Fernholt, L.; Cyvin, B.N.; Sandal, S. *J. Mol. Struct.* **1985**, *128*, 59–76.
[4] Delugeard, Y.; Charbonneau, G.P. *Acta Crystallogr. B* **1977**, *33*, 1586–1588.
[5] Hargreaves, A.; Rizvi, S.H. *Acta Crystallogr. B* **1962**, *15*, 365–373.
[6] Bree, A.; Edelson, M. *Chem. Phys. Lett.* **1977**, *46*, 500–504.
[7] Calleau, H.; Baodour, J.L.; Zeyen, C.M.E. *Acta Crystallogr. B* **1979**, *35*, 426–432.
[8] Barich, D.H.; Pugmire, R.J.; Grant, D.M.; Iuliucci, R.J. *J. Phys. Chem. A* **2001**, *105*, 6780–6784.
[9] Ando, S.; Hironaka, T.; Kurosu, H.; Ando, I. *Magn. Reson. Chem.* **2000**, *38*, 241–250.
[10] Pulham, R.J.; Steele, D. *J. Raman Spectrosc.* **1984**, *15*, 217–223.

[11] Eaton, V.J.; Steele, D. *J. Chem. Soc. Faraday Trans.* **1973**, *2*, 1601.

[12] Charbonnier, S.; Beguemsi, S.T.; N'Guessan, Y.T.; Legoff, D.; Proutiere, A.; Viani, R. *J. Mol. Struct.* **1987**, *158*, 109–125.

[13] Venkataraman, L.; Klare, J.E.; Nuckolls, C.; Hybertsen, M.S.; Steigerwald, M.L. *Nature (London, UK)* **2006**, *442*, 904–907.

[14] Sancho-García, J.C.; Brédas, J.L.; Cornil, J. *Chem. Phys. Lett.* **2003**, *377*, 63–68.

[15] Cacelli, I.; Prampolini, G. *J. Phys. Chem. A* **2003**, *107*, 8665–8670.

[16] Johansson, M.P.; Olsen, J. *J. Chem. Theory Comput.* **2008**, *4*, 1460–1471.

[17] Sizuki, H. *Bull. Chem. Soc. Jpn.* **1959**, *32*, 1340–1350.

[18] Celebre, G.; De Luca, G.; Longeri, M.; Catalano, D.; Veracini, C.A.; Emsley, J.W. *J. Chem. Soc. Faraday Trans.* **1991**, *87*, 2623–2627.

[19] Chandrakumar, T.; Polson, J.M.; Burnell, E.E. *J. Magn. Reson. A* **1996**, *118*, 264–271.

[20] Berardi, R.; Spinozzi, F.; Zannoni, C. *Mol. Cryst. Liq. Cryst.* **1996**, *290*, 245–253.

[21] Catalano, D.; Di Bari, L.; Veracini, C.A.; Shilstone, G.N.; Zannoni, C. *J. Chem. Phys.* **1991**, *94*, 3928–3935.

[22] Sahakyan, A.B.; Shahkhatuni, A.G.; Shahkhatuni, A.A.; Panosyan, H.A. *Magn. Reson. Chem.* **2008**, *46*, 144–149.

[23] Celebre, G.; De Luca, G.; Mazzone, G. *J. Mol. Struct. (THEOCHEM)* **2005**, *728*, 209–214.

[24] Burnell, E.E.; de Lange, C.A. *Chem. Rev.* **1998**, *98*, 2359–2388.

[25] Celebre, G. *J. Chem. Phys.* **2001**, *115*, 9552–9556.

[26] Celebre, G. *Chem. Phys. Lett.* **2001**, *342*, 375–381.

[27] Celebre, G.; De Luca, G.; Emsley, J.W.; Foord, E.K.; Longeri, M.; Lucchesini, F.; Pileio, G. *J. Chem. Phys.* **2003**, *118*, 6417–6426.

[28] Vogel, A.I.; Tatchell, A.R.; Furnis, B.S.; Hannaford, A.J.; Smith, P.W.G. *Vogel's Textbook of Practical Organic Chemistry*; Longman: New York, 1989.

[29] March, J. *Advanced Organic Chemistry*; Wiley: New York, 1992.

[30] Domenici, V.; Czub, J.; Geppi, M.; Gestblom, B.; Urban, S.; Veracini, C.A. *Liq. Cryst.* **2004**, *31*, 91–99.

[31] LiqCryst Online 1999 Database. V. Vill and LCI Publisher, University of Hamburg. http://liqcryst.chemie.uni-hamburg.de/en/lolas.php.

[32] Celebre, G.; De Luca, G.; Longeri, M.; Sicilia, E. *J. Chem. Inf. Comput. Sci.* **1994**, *34*, 539–545.

[33] Celebre, G.; Cinacchi, G. *J. Chem. Phys.* **2006**, 124, 176101 (and references therein).

[34] Emsley, J.W. In *Encyclopedia of NMR*: Grant, D.M., Harris, D.M., Eds.; Wiley: New York, 1996; p 2781.

[35] Celebre, G.; Longeri, M. In *NMR of Ordered Liquids*: Burnell, E.E., de Lange, C.A., Eds.; Kluwer: Dordrecht, 2003.

[36] Brink, D.M.; Satchler, G.R. In *Angular Momentum*: Bleaney, B., Wilkinson, D.H., Eisinger, J., Eds.; Clarendon Press: Oxford, 1971.

[37] Celebre, G.; De Luca, G.; Longeri, M.; Pileio, G.; Emsley, J.W. *J. Chem. Phys.* **2004**, *120*, 7075–7084.

[38] Celebre, G.; Concistré, M.; De Luca, G.; Longeri, M.; Pileio, G. *Chem. Phys. Chem.* **2006**, *7*, 1930–1943.

[39] Concistré, M.; De Lorenzo, L.; De Luca, G.; Longeri, M.; Pileio, G.; Raos, G. *J. Phys. Chem. A* **2005**, *109*, 9953–9963.

[40] Emsley, J.W.; De Luca, G.; Lesage, A.; Merlet, D.; Pileio, G. *Liq. Cryst.* **2007**, *34*, 1071–1093.

[41] Emsley, J.W.; Lesot, P.; De Luca, G.; Lesage, A.; Merlet, D.; Pileio, G. *Liq. Cryst.* **2008**, *35*, 443–464.

[42] Aroulanda, C.; Celebre, G.; De Luca, G.; Longeri, M. *J. Phys. Chem. B* **2006**, *110*, 10485–10496.

[43] Diehl, P. In *NMR of Liquid Crystals:* Emsley, J.W., Ed.; Reidel: Dordrecht, 1985.

[44] Emsley, J.W.; Luckhurst, G.R. *Mol. Phys.* **1980**, *41*, 19–29.

[45] Burnell, E.E.; de Lange, C.A. *J. Magn. Reson.* **1980**, *39*, 461–480.

[46] Burnell, E.E.; de Lange, C.A. *J. Chem. Phys.* **1982**, *76*, 3474–3479.

[47] Burnell, E.E.; de Lange, C.A.; Mouritsen, O.G. *J. Magn. Reson.* **1982**, *50*, 188–196.

[48] Snijders, J.G.; de Lange, C.A.; Burnell, E.E. *J. Chem. Phys.* **1982**, *77*, 5386–5395.

[49] Snijders, J.G.; de Lange, C.A.; Burnell, E.E. *J. Chem. Phys.* **1983**, *79*, 2964–2969.

[50] Lounila, J.; Diehl, P. *Mol. Phys.* **1984**, *52*, 827–845.

[51] Lounila, J.; Diehl, P. *J. Magn. Reson.* **1984**, *56*, 254–261.

[52] Lounila, J. *Mol. Phys.* **1986**, *58*, 897–918.

[53] de Lange, C.A.; Snijders, J.G.; Burnell, E.E. In *Nuclear Magnetic Resonance of Liquid Crystals:* Emsley, J.W., Ed.; Reidel: Dordrecht, 1985; p 181 (and references therein).

[54] Burnell, E.E.; de Lange, C.A.; Barnhoorn, J.B.S.; Aben, I.; Levelt, P.F. *J. Phys. Chem. A* **2005**, *109*, 11027–11036.

[55] Burnell, E.E.; de Lange, C.A. *Solid State Nucl. Magn. Reson.* **2005**, *28*, 73–90.

[56] Burnell, E.E.; de Lange, C.A.; Capitani, D.; Angelini, G.; Ursini, O. *Chem. Phys. Lett.* **2010**, *486*, 21–26.

[57] Emsley, J.W., Ed. *NMR of Liquid Crystals*; Reidel: Dordrecht, 1985.

[58] Grant, D.M.; Harris, D.M., Eds.; *Encyclopedia of NMR*; Wiley: New York, 1996.

[59] Burnell, E.E.; de Lange, C.A., Eds.; *NMR of Ordered Liquids*; Kluwer: Dordrecht, 2003.

[60] Celebre, G.; De Luca, G.; Longeri, M.; Pileio, G. *Mol. Cryst. Liq. Cryst.* **2007**, *465*, 289–299.

[61] Diehl, P.; Bosiger, H.; Zimmermann, H.G. *J. Magn. Reson.* **1979**, *33*, 113–126.

[62] Khetrapal, C.L.; Nagana Gowda, G.A. In *NMR of Ordered Liquids*: Burnell, E.E., de Lange, C.A., Eds.; Kluwer: Dordrecht, 2003.

[63] Emsley, J.W.; Lindon, J.C. *NMR Spectroscopy using Liquid Crystal Solvents*; Pergamon Press: Oxford, 1975.

[64] Pileio, G. Ph.D. Thesis, Department of Chemistry, University della Calabria, 2005.